Comparison of CERES-MODIS and IceSat GLAS Cloud Amounts

Patrick Minnis
NASA Langley Research Center
Hampton, VA 23681

Sunny Sun-Mack, Yan Chen, Q. Z. Trepte, and Yuhong Yi
SSAI
Hampton, VA 23666

Submitted to *Geophysical Research Letters*

February 2008

Abstract

Cloud products from the Ice Cloud and Land Elevation Satellite Geoscience Laser Altimeter System (GLAS) are compared with the fractional cloudiness determined from the *Terra* and *Aqua* Moderate Resolution Imaging Spectroradiometer (MODIS) for the Clouds and Earth's Radiant Energy System (CERES) Project during autumn 2003. GLAS and CERES cloud distributions are very similar, except in polar regions. The GLAS, CERES *Aqua*, and CERES *Terra* global mean cloud fractions are 0.689, 0.613, and 0.609, respectively. In daylight, the three cloud amounts are nearly equal at ~ 0.62. GLAS cloudiness exceeds the CERES values by 0.13 at night because of increased sensitivity. Agreement between GLAS and CERES can be obtained by ignoring all GLAS clouds with optical depths below 0.3, consistent with the expected lower limit of CERES cloud detection. Future CERES improvements should address algorithm inconsistencies over the poles and consistent underestimates of small cumulus and thin cirrus clouds.

1. Introduction

Cloud fractional coverage can vary significantly between different satellite retrievals [e.g., *Zhang et al*., 2005] reinforcing the need to determine their uncertainties and limitations. Validating cloud fractional coverage has been limited to certain locations and times because objective ground-truth measurements are typically taken only at specific well-instrumented ground sites. Because clouds vary greatly in space and time, such limited measurements can be used to verify only a small percentage of the possible cloud conditions. Cloud lidars and radars at those sites provide excellent ground-truth data for passive satellite cloud retrievals. The Ice Cloud and Land Elevation Satellite (ICESat; see *Zwally et al.* [2002]) Geoscience Laser

Altimeter System (GLAS) provides vertical profiles of cloud fraction, cloud-top heights, and cloud optical depths at nadir over the globe [*Spinhirne et al.*, 2005]. Thus, since the launch of ICESat, it has been possible to validate, on the global scale, some cloud properties derived from passive sensors.

Using simultaneous, collocated measurements, *Mahesh et al.* [2004] found 75% agreement in the clear and cloudy categories as determined from GLAS 1064-nm data and 1-km *Terra* and *Aqua* Moderate Resolution Imaging Spectroradiometer (MODIS) by the MODIS Atmospheres Team [*Ackerman et al.*, 2002]. Because ICESat is in a different orbit than either *Terra* or *Aqua*, collocated sampling with GLAS is relatively sparse, limited primarily to higher latitudes. To overcome the sampling discrepancies, *Wylie et al.* [2007] compared GLAS mean cloud amounts with those derived from High Resolution Infrared Sounder (HIRS) data taken during the same time period. The HIRS yielded 7% more cloudiness relative to that from GLAS, mainly due to overestimates in polar regions and the effects of the HIRS large footprint.

Clouds amounts have also been derived from MODIS data using algorithms developed for the Clouds and Earth's Radiant Energy System (CERES; *Wielicki et al.*, [1998]). These cloud properties, matched closely with CERES-measured radiative fluxes, are critical for understanding the relationships between the Earth's radiation budget and cloudiness. To provide an initial estimate of their uncertainties and limitations over the globe, this paper compares the CERES-MODIS cloud amounts with those from GLAS.

2. Data and Comparison Methodology

During January 2003, ICESat was launched into a 94° inclined orbit that precesses ~0.5°/day relative to a Sun-synchronous orbit. The GLAS lasers operate at 1064 and 532 nm at 40 Hz with

footprints that are ~70 m wide and spaced at ~176 m. The latter channel was designed specifically for detecting clouds and aerosols and detects about twice many clouds with optical depths (OD) less than 0.25 as the 1064-nm channel [*Spinhirne et al.*, 2005]. Cloud layers are identified using the updates of the algorithms described by *Palm et al.* [2002], *Hart et al.* [2005], *Hlavka et al.* [2005], and *Spinhirne et al.* [2005]. Cloud detection is performed at full resolution and for signals averaged at 0.2, 1, and 4-s intervals. The mid-resolution or 1-s averages, equivalent to 7.1-km long and 0.07-km wide pixels, are used here. Cloud OD, is determined for a column of cloud layers having a cumulative OD < 3.0, is reliably measured down to values $\leq$ 0.02.

The GLAS lasers experienced some technical problems [*Abshire et al.*, 2005] that required operating the lasers only during three 33-day periods each year [*Schutz et al.*, 2005]. Additionally, the 532-nm laser only operated satisfactorily during the GLAS L2a campaign from 25 September through 18 November 2003, the period used here. It was turned off during 25 September and 7 October, time periods excluded from the averaging. The 1064-nm cloud product was not used because of its reduced sensitivity and discrimination between aerosols and clouds requires both channels. Specifically, the 1-Hz R028 version of GLA09 Level 2 Global Cloud Heights Including Multiple Layers dataset is used to define the cloud boundaries through the atmosphere from top to bottom for all clouds. If a cloud layer is detected, the "pixel" is considered cloudy and the cloud fractional coverage within a 2° x 2° region is computed for a given overpass, if more than 1 pixel falls within the area boundaries. Regional and zonal averages were computed using the results of each overpass for the entire period.

Sampling within a given region varies with latitude; the greatest number of samples occurs near 77° latitude where cloud fraction was measured more than 130 times in a given region. In

the Tropics, the number varied from 48 to 83. During the day, the number of regional samples exceeded 30 south of 30°N, ranged from 15-30 for 30°N – 60°N, and dropped to 0 - 15 poleward of 60°N. At night (all times with solar zenith angles less than 82°), the sampling was between 30 and 50 south of 30°N, increased to ~50 between 30 and 60°N, and exceeded 60 for points north of 60°N. This asymmetric day-night sampling results from the time of year and near-terminator ICESat orbit at that time.

The CERES-MODIS, hereafter referred to as CERES, cloud data analyzed here consist of 1° x 1° cloud fractions computed from the CERES *Terra* Edition2B and *Aqua* Edition1A 1-km pixel-level results. *Terra* and *Aqua* are both in Sun-synchronous orbits with equatorial crossing times of 1030/2230 and 0130/1330 LT, respectively. These can be compared to the GLAS crossing times, which ranged from 0818/2018 on 25 September 2003 to 0655/1855 LT on 18 November 2003. The CERES cloud subsystem analyzed every other pixel and every fourth scan line of the 1-km MODIS Collection-4 data. Each pixel is classified as either clear or cloudy using algorithms for non-polar [*Minnis et al.*, 2008] and polar [*Trepte et al.*, 2002] regions. Pixel-level results serve as input to the CERES Single Scanner Footprint (SSF) product that combines CERES 20-km broadband flux measurements with the coincident, 1-km MODIS cloud and aerosol retrievals [*Geier et al.*, 2003]. Pixel-level results are only retained over selected regions for quality control and special studies. During processing, however, 1° x 1° averages of every cloud parameter are computed for each overpass for quality control. For this study, the 1° means were further averaged over 2° x 2° regions corresponding to those used for the GLAS averaging. Zonal and regional mean cloud amounts were also computed.

3. Results

The mean cloud fractions from the three satellites and some of their differences are shown in Figure 1. The overall patterns in mean cloud fraction (Figure 1a, c, d) from all three datasets are very similar but, in certain areas, differ significantly in magnitude. The GLAS cloud amounts are generally less than those from *Aqua* over Antarctica, but are greater over the Arctic (Figure 1e), where a discontinuity occurs around 60°N due to change from the polar to non-polar mask. Similarly, *Terra* underestimates Arctic cloud amounts compared to GLAS (Figure 1f), but yields the same cloud fraction as GLAS over Antarctica (Figure 1b). In many other areas, the GLAS–CERES differences range between -0.1 and 0.1.However, over marine areas dominated by trade cumulus and deep convection, CERES underestimates cloud amount by up to 0.40. Over land, the differences are as large as 0.25, especially between 45°N and 60°N.

Figure 2 provides a surface-type breakdown of the CERES-GLAS zonal differences for both *Aqua* (Figure 2a) and *Terra* (Figure 2b). The mean differences (solid symbols) approach 0.24 and 0.28 at 82.5°N for *Aqua* and *Terra*, respectively. At the other end of the globe, the differences for *Aqua* are -0.16. The *Terra* differences over land generally exceed those over ocean with values frequently greater than 0.1. The *Aqua* differences over land are less than their tropical ocean and *Terra* counterparts. Over ice-free water, the largest differences, ~ 0.12, are over the Tropics. Good agreement occurs over the southern oceans, especially for *Terra*.

The differences depend on time of day (Figure 3). Between 0° and 70°N, the mean CERES and GLAS cloud amounts are typically within ±0.04 of the GLAS values, but at night, the average difference is ~0.18. This day-night discrepancy is much smaller between 30°S and 60°S. The Arctic measurements were nearly always taken at night, so the differences are similar to those in Figure 2. The *Terra* differences over Antarctica are small during daylight and overestimated at night. Since most Antarctic sampling is during daylight, the mean difference is

close to zero (Figure 2b). On the other hand, the corresponding *Aqua* differences are negative during the day and positive at night.

On average, the GLAS global cloud amount is 0.078 greater than the CERES values (Table 1). The GLAS mean global cloud fraction, 0.689, is 0.014 less than that reported by *Wylie et al.* [2007], who used the R026 version of the GLAS products. The more recent R028 version used here yields slightly smaller cloud fractions during both day and night. During daytime, the mean GLAS cloud fraction is only 0.015 greater than the CERES values, but at night, the difference jumps to 0.132.

4. Discussion

Presumably, the GLAS cloud amounts are the most accurate estimate of global cloud cover for the period. However, their accuracy is compromised at the regional scale because of sampling. During L2a, each GLAS overpass sampled a very small portion of each 2 ° x 2° region, approximately 65 times in the Tropics and much more near the poles. MODIS sampled nearly all areas ~80 times over the Tropics and more than 500 times near the poles. The impact of sampling differences is evident in the chunkiness of the cloud fields in Figure 1a where the averages in areas that should be relatively uniform change by 0.1 or more from one region to the next. Except for areas with either extremely large (e.g., 50°S) or small (e.g., Sahara) cloud fractions, the standard deviation of the CERES regional cloud amounts during the period divided by the square root of the number of GLAS samples is ~ 0.1. Thus, GLAS-CERES differences between ±0.1 are likely to be within the uncertainty of the GLAS averages. Otherwise, the regional difference is statistically significant. Assuming a regional mean cloud fraction

uncertainty of 0.1, the GLAS zonal averages should be accurate to better than ±0.01. Thus, it is clear that, on average, the CERES cloud amounts are too low.

The *Aqua* and *Terra* discrepancies arise from several factors: sampling times, calibration differences, and algorithmic changes. Cloud amounts over marine stratus areas are likely to be greater from *Terra* because it samples nearer the peak of the diurnal cycle (e.g., *Minnis and Harrison* [1984]) than *Aqua*, which samples near the daytime bottom of the cycle and well below the peak at night. The near-terminator GLAS average would likely be closer to *Terra* than to *Aqua*. This diurnal effect is evident in Figure 2 where the *Aqua* differences are greater than *Terra's* between 30 and 60° latitude. The *Terra* orbit was selected to minimize cloud cover over land. Hence, it is expected that, over many land areas, *Aqua* should yield greater cloud amounts. This is reflected in the non-polar differences (Figure 2). The diurnal variations in actual cloud cover also contribute to the day-night differences between *Terra* and *Aqua* in Table 1.

Differences in the MODIS 0.64-µm and 3.8-µm channel calibrations [*Minnis et al.*, 2008a,b] would produce only negligible differences in cloud amounts during the day, but at night, the 3.8-µm channel could produce greater differences in cloud amounts between the satellites where the surface temperature is less than 250 K. Thus, any discrepancies between the *Aqua* and *Terra* nighttime differences in polar regions are, in part, due to calibration differences. However, the extreme divergence between the *Aqua* and *Terra* differences over Antarctica is primarily due to algorithmic changes. The *Terra* daylight algorithm depends heavily on the 1.6-µm channel and, over cold high plateaus (e.g., Antarctica), uses a 6.7-µm minus 11-µm brightness temperature difference test to help detect clouds. This cold plateau test was not used during daytime for *Aqua*. The 1.6-µm channel, unavailable on *Aqua*, was replaced with the 2.1-µm channel in the polar algorithm. An empirical adjustment was applied to the 1.6-µm clear snow albedo model used for

Terra to estimate the 2.1-μm clear snow albedo. For *Aqua*, thresholds in specific spectral tests were adjusted from their *Terra* values apparently causing overestimates of Antarctic daytime cloud cover. At night, *Aqua* employed the cold plateau test, but the thresholds were adjusted to account for *Terra's* overestimated Antarctic nocturnal cloudiness. Apparently, the adjustments were too large resulting in an underestimate of nighttime cloudiness by *Aqua* (Figure 3).

Although the CERES cloud fraction is relatively constant diurnally, the underestimate of cloud fraction by CERES is mainly confined to nighttime. During daytime, the CERES polar cloud overestimates tend to balance the shortfall in the southern Tropics (Figure 3). Two other daytime algorithm changes, improved thin cirrus and sunglint detection tests, were employed in *Aqu*a Edition1A. These can partially explain the reduced differences relative to *Terra* in the Tropics where thin cirrus clouds are common. Except for the polar regions, the two CERES underestimates at night are fairly close suggesting that there is an actual dramatic increase in global cloud cover at night, the GLAS retrieval is more sensitive at night, or both. During the daytime, sunlight produces much noisier GLAS returns than during the night [*Spinhirne et al.*, 2005]. Subsequently, GLAS should detect more clouds at night. This expectation is confirmed by the fraction of clouds having OD < 0.1 increasing from 0.034 during daytime to 0.068 at night. Other clouds with larger optical depths must also increase at night to account for the 0.119 day-night difference in GLAS cloudiness.

The CERES cloud mask generally fails to detect clouds with OD < 0.3 [e.g., *Chiriaco et al.*, 2007]. To determine how this limitation affects the GLAS–CERES comparisons, the mean GLAS cloud amounts were recomputed ignoring all clouds having a cumulative OD less than a certain amount. If all GLAS clouds with OD $\leq$ 0.3 are ignored (Figure 4a), the cloud distribution looks much more like that from *Terra* (Figure 1d), except over the Arctic. The zonal differences

between all GLAS cloud amounts and those for OD > 0.1, 0.3, and 3.0 peak in the Tropics and near the poles. Eliminating those with OD $\leq$ 0.3 would account for nearly all of the clouds missed over the Tropics by CERES (Figure 3), but CERES would still underestimate (overestimate) cloud cover over the Arctic (Antarctica). Globally, the mean GLAS cloud amounts are 0.639, 0.611, and 0.515 when only clouds with OD > 0.1, 0.3, and 3.0 are included. Thus, it is clear CERES detects clouds quite well in non-polar regions when OD > 0.3.

The remaining undetected cloud cover has a mean optical depth of 0.13. Those clouds are not necessarily all cirrus clouds. For example, the cloud cover over trade cumulus areas in Figure 4a is reduced significantly compared to that in Figure 1a. These correspond to many of the tropical red regions in Figure 1f. Determining the error in CERES cloud radiative forcing as a result of missing these clouds will require height information as well as the optical depth and cloud fraction of the missing clouds.

5. Conclusions

The CERES cloud detection algorithms produce reasonably accurate cloud amounts over non-polar areas during both day and night for most clouds having optical depths greater than 0.3. At night, the GLAS detects many more clouds than during the day. This additional, presumably thin, cloud cover is not detected by CERES. Over the Arctic at night, the CERES *Terra* and *Aqua* cloud amounts are in relatively good agreement, but underestimate the cloudiness by ~0.14, on average. Differences in the cloud algorithms and the MODIS calibration give rise to large discrepancies between the *Terra* and *Aqua* results over Antarctica. Some major problems revealed in this study should be addressed in future editions of the CERES cloud algorithms. These include the *Terra-Aqua* inconsistencies, large underestimates of polar cloudiness and trade

cumulus, polar discontinuities, and thin cirrus. With the aid of datasets like those from GLAS, such improvements are possible.

Acknowledgements

This research was supported by the NASA Science Mission Directorate through the ICESat Program and the CERES Project. Thanks to Jim Spinhirne and Steve Palm for assistance with interpreting the GLAS data.

References

Abshire, J. B., X. Sun, H. Riris, J. M. Sirota, J. F. McGarry, S. Palm, D. Yi, and P. Liiva (2005), Geoscience Laser Altimeter System (GLAS) on the ICESat Mission: On-orbit measurement performance, *Geophys. Res. Lett*., *32*, L21S02, doi:10.1029/2005GL024028.

Ackerman, S. A., K. I. Strabala, W. P. Menzel, R. A. Frey, C. C. Moeller, and L. E. Gumley (1998), Discriminating clear-sky from clouds with MODIS, *J. Geophys. Res.*, *103(D24)*, 32,141– 32,157.

Chiriaco, M., and Co-authors (2007), Comparison of CALIPSO-like, LaRC, and MODIS retrievals of ice cloud properties over SIRTA in France and Florida during CRYSTAL-FACE, *J. Appl. Meteorol. Climatol.*, *46*, 249-272.

Cohen, S., J. Degnan, J. Bufton, J. Garvin, and J. Abshire (1987), The Geoscience Laser Altimetry/ranging system, *IEEE Trans. Geosci. Remote Sens.*, *GE-25*, 581– 592.

Geier, E. B., R. N. Green, D. P. Kratz, P. Minnis, W. F. Miller, S. K. Nolan, and C. B. Franklin, (2003), Clouds and the Earth's Radiant Energy System Data Management System Single Satellite Footprint TOA/Surface Fluxes and Clouds (SSF) Collection Document, Release 2,

Version 1, 243 pp. (http://asd-www.larc.nasa.gov/ceres/collect_guide/SSF_CG.pdf).

Mahesh, A., M. A. Gray, S. P. Palm, W. D. Hart, and J. D. Spinhirne (2004), Passive and active detection of clouds: Comparisons between MODIS and GLAS observations. *Geophys. Res. Lett.*, *31*, L04108, doi: 10.1029/2003GL018859.

Minnis, P. and E. F. Harrison (1984), Diurnal variability of regional cloud and clear-sky radiative parameters derived from GOES data, Part II: November 1978 cloud distributions, *J. Clim. Appl. Meteorol.*, *23*, 1012-1031.

Minnis, P., D. R. Doelling, L. Nguyen, W. F. Miller, and V. Chakrapani (2008b), Assessment of the visible channel calibrations of the TRMM VIRS and MODIS on *Aqua* and *Terra*, *J. Atmos. Oceanic Technol*., in press.

Minnis, P., and Co-authors (2008a), Cloud detection in non-polar areas for CERES using TRMM VIRS and Terra and Aqua MODIS data, submitted to *IEEE Trans. Geosci. Remote Sens*.

Palm, S. P., J. D. Spinhirne, W. D. Hart, D. L. Hlavka, E. J. Welton, and A. Mahesh (2002), Geoscience Laser Altimeter System algorithm theoretical basis document: Atmospheric data products. [Available online at http://www.csr.utexas.edu/glas/pdf/glasatmos.atbdv4.2.pdf.]

Randall, D., B. Albrecht, S. Cox, D. Johnson, P. Minnis, W. Rossow, and D. Starr (1996), On FIRE at ten, *Adv. Geophys., 38*, 37-177.

Schutz, B. E., H. J. Zwally, C. A. Shuman, D. Hancock, and J. P. DiMarzio (2005), Overview of the ICESat Mission, *Geophys. Res. Lett.*, *32*, L21S01, doi:10.1029/2005GL024009.

Spinhirne, J. D., S. P. Palm, W. D. Hart, D. L. Hlavka, and E. J. Welton (2005), Cloud and aerosol measurements from GLAS: Overview and initial results, *Geophys. Res. Lett.*, *32*, L22S03, doi: 10.1029/2005GL023507.

Trepte, Q., P. Minnis, and R. F. Arduini (2002), Daytime and nighttime polar cloud and snow identification using MODIS data. *Proc. SPIE 3rd Intl. Asia-Pacific Environ. Remote Sensing Symp. 2002: Remote Sens. of Atmosphere, Ocean, Environment, and Space*, Hangzhou, China, October 23-27, Vol. 4891, 449-459.

Wielicki, B. A, B. R. Barkstorm, E. F. Harrison, R. B. Lee III, G. L. Smith, and J. E. Cooper (1996), Clouds and the Earth's Radiant Energy System (CERES): An Earth Observing System Experiment, *Bull. Am. Meteorol. Soc.*, *77*, 853-868.

Wylie, D., E. Eloranta, J. D. Spinhirne, and S. P. Palm (2007) Comparison of cloud cover statistics from the GLA lidar with HIRS, *J. Climate*, *20*, 4968-4981.

Zhang, M. H., and Co-authors (2005), Comparing clouds and their seasonal variations in 10 atmospheric general circulation models with satellite measurements, *J. Geophys. Res.*, *110*, 10.1029/2004JD005021.

Zwally, H. J., et al. (2002), Ice, cloud and land elevation satellite's laser measurements of polar ice, atmosphere, ocean and land, *J. Geodyn.*, *34*, 405– 445.

Figure Captions.

Figure 1. Average cloud fractions and differences, 26 September – 18 November 2003. (a) GLAS cloud fraction. (b) Zonal averages. CERES cloud fractions from (c) *Aqua* and (d) *Terra*. GLAS - CERES cloud fraction differences from (e) *Aqua* and (f) *Terra*.

Figure 2. GLAS – CERES mean zonal cloud fraction differences from (a) *Aqua* and (b) *Terra*, 26 September – 18 November 2003.

Figure 3. GLAS – CERES mean zonal, day and night cloud fraction differences from *Aqua* and *Terra*, 26 September – 18 November 2003.

Figure 4. Dependence of GLAS cloud fractions on cloud optical depth, 26 September – 18 November 2003. (a) GLAS cloud fraction for all clouds with OD > 0.3. Compare to Figure 1a. (b) Zonal differences between GLAS average cloud fraction and for all GLAS clouds having optical depths exceeding 0.1, 0.3, and 3.

Table 1. Comparison of CERES and GLAS cloud amounts, 26 September – 18 November 2003. Numbers in parentheses refer to GLAS version R026.

	Day	Night	Total
GLAS 532	62.8 (63.2)	74.1 (74.4)	68.9 (70.3)
CERES Aqua	62.0	60.6	61.3
CERES Terra	60.5	61.3	60.9

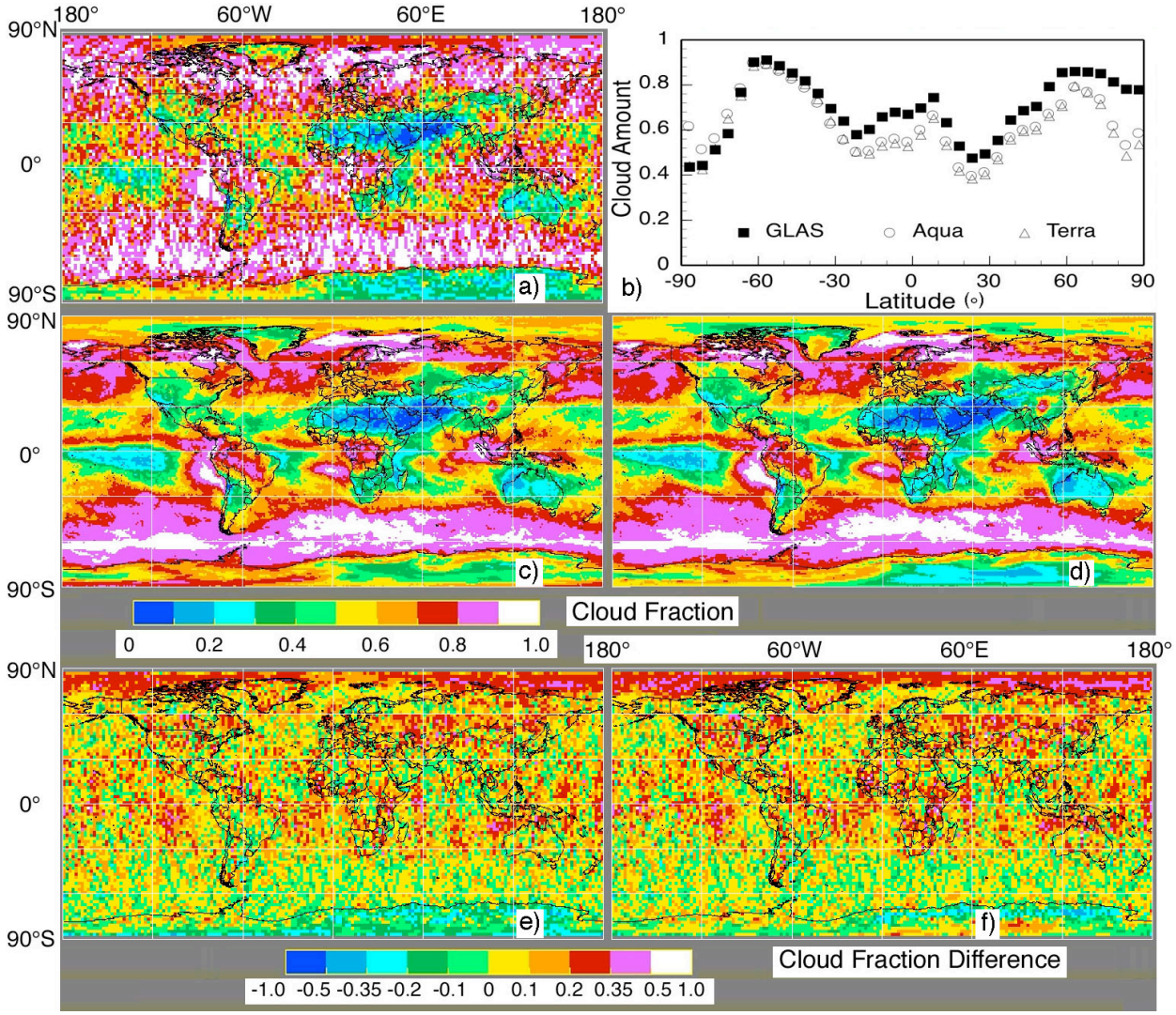

Figure 1. Average cloud fractions and differences, 26 September – 18 November 2003. (a) GLAS cloud fraction. (b) Zonal averages. CERES cloud fractions from (c) *Aqua* and (d) *Terra*. GLAS - CERES cloud fraction differences from (e) *Aqua* and (f) *Terra*.

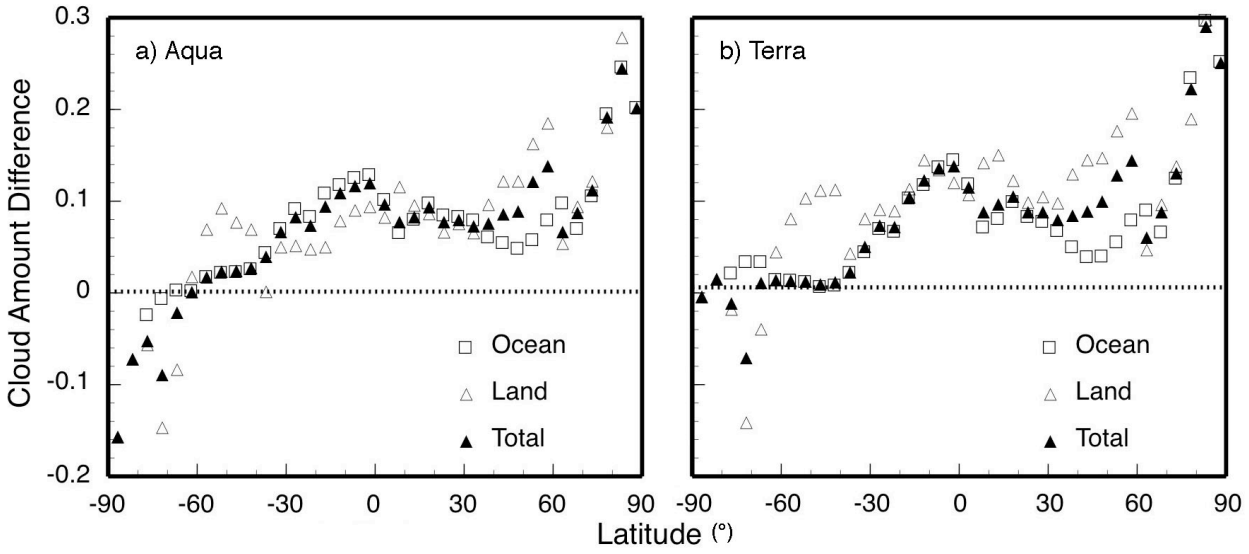

Figure 2. GLAS – CERES mean zonal cloud fraction differences from (a) *Aqua* and (b) *Terra*, 26 September – 18 November 2003.

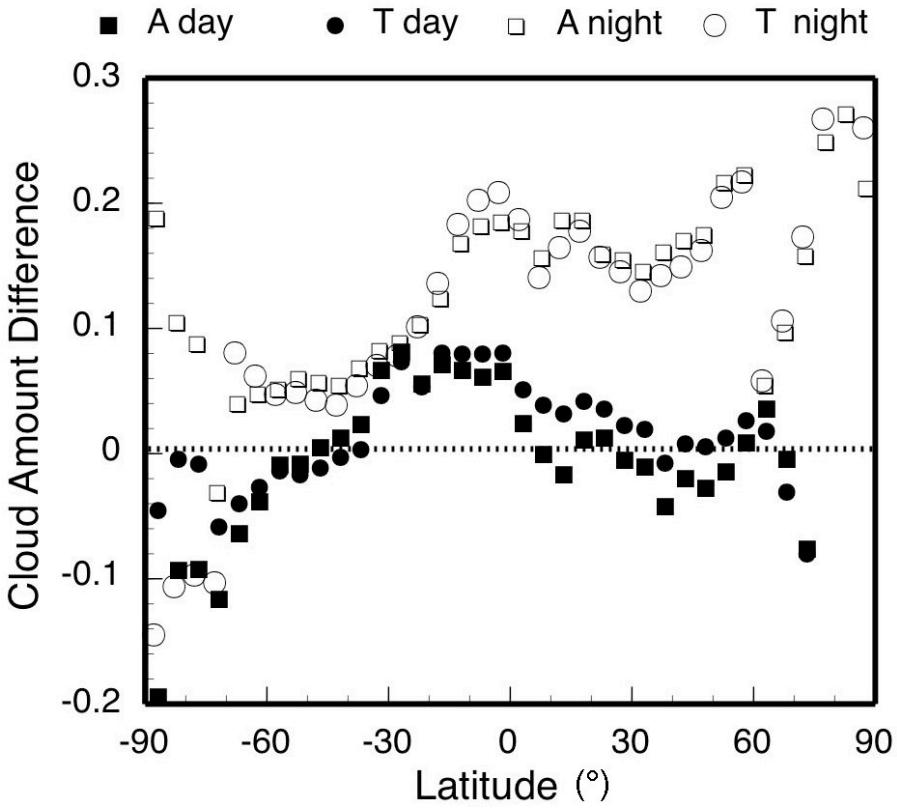

Figure 3. GLAS – CERES mean zonal, day and night cloud fraction differences from *Aqua* and *Terra*, 26 September – 18 November 2003.

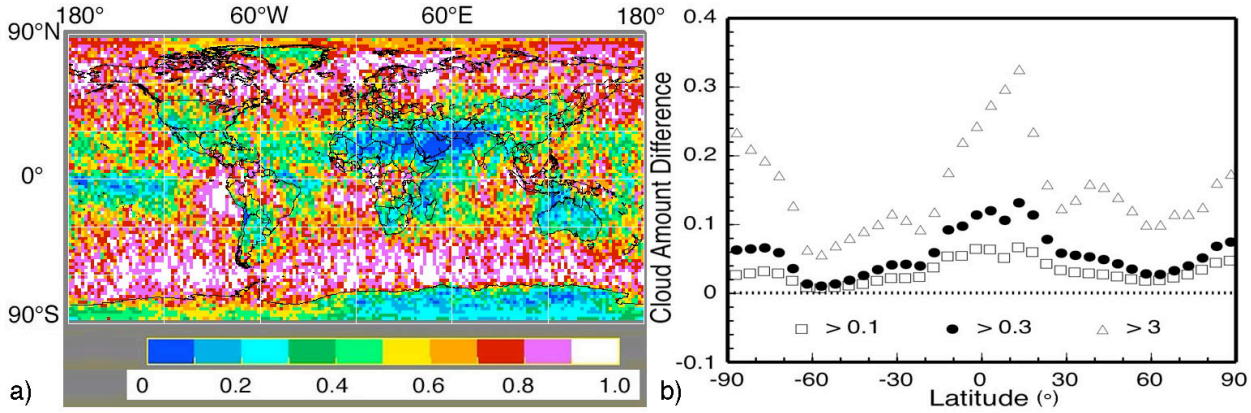

Figure 4. Dependence of GLAS cloud fractions on cloud optical depth, 26 September – 18 November 2003. (a) GLAS cloud fraction for all clouds with OD > 0.3. Compare to Figure 1a. (b) Zonal differences between GLAS average cloud fraction and for all GLAS clouds having optical depths exceeding 0.1, 0.3, and 3.